Catal Lett (2008) 124:91–99
DOI 10.1007/s10562-008-9429-1

Highly Active $La_{1-x}K_xCoO_3$ Perovskite-type Complex Oxide Catalysts for the Simultaneous Removal of Diesel Soot and Nitrogen Oxides Under Loose Contact Conditions

Hong Wang · Zhen Zhao · Peng Liang · Chunming Xu · Aijun Duan · Guiyuan Jiang · Jie Xu · Jian Liu

Received: 27 October 2007 / Accepted: 7 February 2008 / Published online: 27 February 2008

Abstract The nanometric $La_{1-x}K_xCoO_3$ ($x = 0$–0.30) perovskite-type oxides were prepared by a citric acid-ligated method. The catalysts were characterized by means of XRD, IR, BET, XPS and SEM. The catalytic activity for the simultaneous removal of soot and nitrogen oxides was evaluated by a technique of the temperature-programmed oxidation reaction. In the $LaCoO_3$ catalyst, the partial substitution of La^{3+} at A-site by alkali metal K^+ enhanced the catalytic activity for the oxidation of soot particle and reduction of NO_x. The $La_{0.70}K_{0.30}CoO_3$ oxides are good candidate catalysts for the simultaneous removal of soot particle and NO_x. The combustion temperatures for soot particles over the $La_{0.70}K_{0.30}CoO_3$ catalyst are in the range from 289 to 461 °C, the selectivity of CO_2 is 98.4% and the conversion of NO to N_2 is 34.6% under loose contact conditions. The possible reasons that can lead to the activity enhancement for the K-substitution samples compared to the unsubstituted sample ($LaCoO_3$) were given. The particle size has a large effect on its catalytic performance for the simultaneous removal of diesel soot and nitrogen oxides.

H. Wang · Z. Zhao (✉) · C. Xu · A. Duan · G. Jiang · J. Xu · J. Liu
State Key Laboratory of Heavy Oil Processing, China University of Petroleum, Beijing 102249, China
e-mail: zhenzhao@cup.edu.cn

H. Wang
Beijing Institute of Petrochemical Technology, Beijing 102617, China

P. Liang
Material Science & Chemical Engineering School, Eastern Liaoning University, Dandong, Liaoning 118003, China

Keywords Perovskite-type oxides · Diesel soot · Nitrogen oxides · Potassium · Catalysts · Simultaneous removal

1 Introduction

Particulate matter mainly containing soot and NO_x are the main pollutants in diesel engine emissions. The combination of a filter with oxidation catalysts appears to be the most plausible after-treatment technique to eliminate soot particles. Since the temperature in the exhaust gases may be as low as 200 °C for small engines, and can exceed 600 °C at full load for heavy engines [1], a useful catalyst has to be operated efficiently at low temperatures and to be thermally stable.

Several authors [2–5] reported that perovskite-type oxides are active for the simultaneous removal of NO_x and soot reaction. In addition, the substitutional incorporation of K into A-sites of perovskite-type (ABO_3) oxides was found to be quite effective in enhancing the activity and selectivity for the NO_x–O_2-soot reaction [4–8]. However, the reasons that can lead to the activity enhancement for the alkali metal substitution are not fully understood. Teraoka et al. found that La–K–Co–O_3 [3] and La–K–Mn–O_3 [8] perovskite-type oxides are good catalysts for the simultaneous removal of diesel soot and NO_x, but they reported the relevant catalytic activities under tight conditions between catalysts and soot particle. However, under practical conditions the contact between the catalysts on the surface of filter and PM particle is loose [9, 10]. Therefore, it is rather significant to study and develop active catalysts for the title reactions under loose contact conditions.

Though the La–K–Co–O_3 catalyst itself is not a new catalyst system for the simultaneous removal soot and NO_x,

it is still important to study the catalyst on this reaction under loose contact conditions. In this work, nanometric $La_{1-x}K_xCoO_3$ perovskite oxide catalysts were prepared, characterized, and their catalytic activitives for title reaction were tested under loose contact conditions. It has been found that the nanometric $La_{1-x}K_xCoO_3$ perovskite oxides are good candidate catalysts for the simultaneous removal of diesel soot particle and NO_x reaction under loose contact conditions. The probable reasons that can lead to the activity enhancement for the K-substituted samples compared to the unsubstituted sample ($LaCoO_3$) were discussed. In order to investigate the particle size effect on the title reaction, the samples with different particles sizes were also obtained by different preparation methods and their catalytic performances were also evaluated for comparison.

2 Experimental

2.1 Catalyst Preparation

A series of $La_{1-x}K_xCoO_3$ ($x = 0$–0.30) perovskite-type oxide samples were prepared by the citric acid-ligated method, starting from aqueous solution of various salts (e.g. $La(NO_3)_3$, $Co(NO_3)_2$, KNO_3, etc.), followed by heating and evaporating to dryness with vigorous stirring, and burning or exploding and finally the precursor was calcined at 800 °C for 6 h in static air. For safety the ceramic evaporation pottery with wide open mouth was used for the drying of the resulting solution and this drying process was carried out inside a hood. This technique is particularly suited to produce nanosized particle samples. For comparison, the $La_{0.9}K_{0.1}CoO_3$ samples with different particle sizes were further treated. They were compressed at 10 MPa, followed by sieving, then obtained the sample sizes of 180–230 μm and 380–830 μm, respectively. Moreover, the $La_{0.9}K_{0.1}CoO_3$ sample was also prepared by the solid phase mechanically mixed method. The La_2O_3, CoO, and KNO_3 were mechanically milled 30 min and calcined at 800 °C for 6 h in static air.

2.2 Catalyst Characterization

The BET specific surface area of the studied samples was measured with linear parts of the BET plot of the N_2 isotherms, using a Micromeritics ASAP 2010 analyzer. The morphologies of the catalysts were observed by SEM instrument (Hitachi S-4300, Japan). XRD spectra of fresh catalysts were collected on a Shimadzu XRD 6000 diffractometer using Cu Kα ($\lambda = 1.54184$ Å) to verify perovskite-type crystal structure. Spectra were recorded for 2θ values from 5° to 80° at a scanning rate of 4°/min. FT-IR spectra were recorded on a Digilab FTS-3000 spectrophotometer. The measured wafer was prepared as KBr pellet with the weight ratio of sample to KBr, 1/100. The resolution was set at 2 cm^{-1} during measurement. The XPS spectra were obtained using an ESCALAB MKII Physical Electronics Photoelectron Spectrometer with monochromatized Al Kα X-ray radiation. A power of 250 W and a pass energy of 37.5 eV was used during the experiments. The base pressure of the analysis chamber was better than 5×10^{-9} Torr. All the spectra were calibrated using the binding energy of C1s (284.6 eV) as reference.

2.3 Activity Test

The catalytic activity for the combustion of soot was determined by temperature-programmed reaction (TPR). A gaseous flow (50 cm^3/min) with 5% oxygen and 2,000 ppm NO in helium was used and the temperature was increased at a rate of 2 °C/min using 180 mg mixture of the catalyst and soot (5:1), mixed with a spatula in order to reproduce the loose contact mode [11, 12]. A modified TPR technique [13] was employed which consists of passing the gases coming from the reactor through a methanation reactor, where CO and CO_2 were converted into CH_4. Afterwards, methane was measured with an FID detector. The methanation reactor contained a nickel catalyst, and operated at 380 °C. The N_2 and O_2 in the gas from the reactor were measured with a TCD detector. In all TPR experiments, temperatures were increased until the soot was completely burnt off.

3 Results and Discussion

3.1 BET Results

The specific surface areas of the $La_{1-x}K_xCoO_3$ catalysts are listed in Table 1. The BET surface areas of this system of complex oxide catalysts are between 9 and 12 m^2/g.

Table 1 Specific surface area of the $La_{1-x}K_xCoO_3$ catalysts

Catalyst	BET (m^2/g)
$LaCoO_3$	9.0
$La_{0.95}K_{0.05}CoO_3$	10.8
$La_{0.90}K_{0.10}CoO_3$	11.1
$La_{0.85}K_{0.15}CoO_3$	11.6
$La_{0.80}K_{0.20}CoO_3$	10.4
$La_{0.75}K_{0.25}CoO_3$	9.9
$La_{0.70}K_{0.30}CoO_3$	9.7
$La_{0.90}K_{0.10}CoO_3$ (180–230 μm)	12.0
$La_{0.9}K_{0.1}CoO_3$ (solid phase mechanically mixed method, 180–230 μm)	5.1

The change of the BET surface area is not obvious after the sample being compressed and sieved. The BET surface area of the sample of the solid phase mechanically mixed method is lower (5.1 m^2/g) than that of the sample prepared by the citric acid-ligated method. It may also affect its catalytic performance.

3.2 XRD Results

The XRD patterns of the $La_{1-x}K_xCoO_3$ ($x = 0$–0.30) perovskite-type oxides are shown in Fig. 1. The diffraction peaks of $LaCoO_3$ are in good agreement with the JCPDS 25-1060 file, which corresponds to a rhombohedral system. All the characteristic diffraction peaks, which belong to $LaCoO_3$, were observed in the spectra of all the K-substituted samples indicating that the complex oxides of $La_{1-x}K_xCoO_3$ ($x = 0$–0.30) possessed ABO_3 perovskite-type structures with rhombohedral symmetry. Very weak peaks at 2θ value of $\sim 37°$ or $\sim 66°$ appeared when K-substitution amount is higher than 0.1 suggesting that a small amount of Co_3O_4 was formed when large amount of La^{3+} was replaced by K^+. For comparison, the XRD pattern of the $La_{0.9}K_{0.1}CoO_3$ sample prepared by the solid phase mechanically mixed method is shown in Fig. 2. The result indicates that the sample obtained by different preparation method also formed perovskite structure.

3.3 FT-IR Results

BO_6 octahedron, which has A-site cation in their clearance, is the repeatable structure unit of ABO_3 crystalline structure. There are six kinds of vibrations to their IR spectra, and the stretching vibration (v_3) is IR inactive if three pairs of B–O bonds have the same length, i.e., BO_6 octahedron having high symmetry. On the contrary, the B–O stretching vibration v_3 is IR active if the symmetry of BO_6 is low [14].

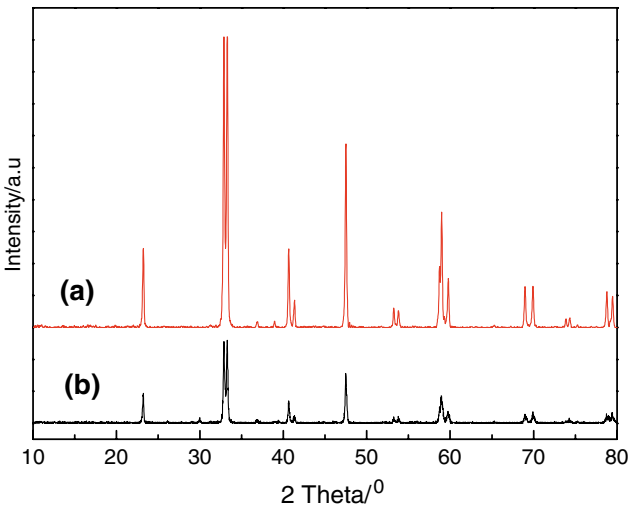

Fig. 2 X-ray diffraction patterns of $La_{0.9}K_{0.1}CoO_3$ catalysts prepared by the different methods. (**a**) Citric acid-ligated method, (**b**) solid phase mechanically mixed method

Figure 3 shows the IR spectra of $La_{1-x}K_xCoO_3$ ($x = 0$–0.30) perovskite-type oxides. There are three vibration bands, at 424, 562, and 596 cm^{-1}, in the IR spectra of all $La_{1-x}K_xCoO_3$ samples. The vibration band at 424 cm^{-1} belongs to the bending vibration of Co–O bonding in the BO_6 octahedron, and the bands at 562 and 596 cm^{-1} can be assigned to two kinds of Co–O bond stretching vibration in the BO_6 octahedron [15, 16]. These results further prove that the complex oxides of $La_{1-x}K_xCoO_3$ ($x = 0$–0.30) possessed ABO_3 perovskite-type structures. Compared to unsubstituted sample $LaCoO_3$, the band at 596 cm^{-1} become broad and upshifting suggesting that some amounts of Co^{3+} changed into Co^{4+} when some La^{3+} were replaced by K^+. The interaction between Co^{4+} and O is stronger than that of Co^{3+} and O, and thus the wave number of the stretching vibration of Co^{4+}–O is

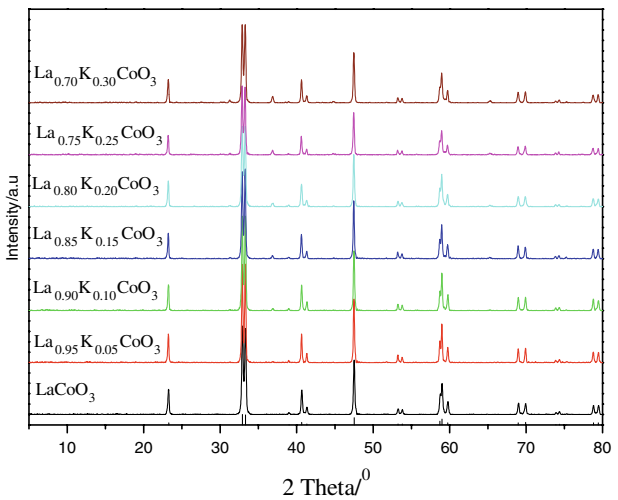

Fig. 1 X-ray diffraction patterns of $La_{1-x}K_xCoO_3$ catalysts

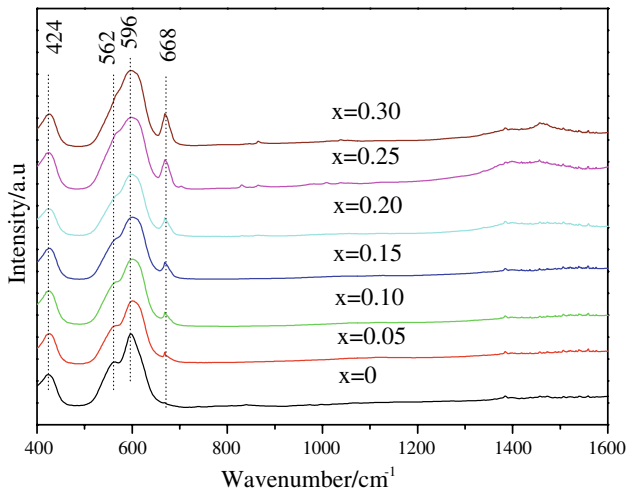

Fig. 3 FT-IR spectra of $La_{1-x}K_xCoO_3$ catalysts

greater than that of Co^{3+}–O. Therefore, the upshifting of the wave number of stretching vibration of Co–O bond in the BO_6 octahedron may suggest the formation of some Co^{4+}.

A very weak new vibration band at 668 cm^{-1}, which has been assigned to the Co_3O_4, appeared when some amounts of K^+ were introduced to partially replace La^{3+} in $LaCoO_3$ and its' intensity gradually increased with increasing K^+ substitution amount. These results indicate again that a small amount of Co_3O_4 was formed when some amounts of La^{3+} were replaced by K^+. The IR results are very consistent with the XRD analysis.

3.4 SEM Results

SEM photographs of the $LaCoO_3$, $La_{0.95}K_{0.05}CoO_3$ and $La_{0.90}K_{0.10}CoO_3$ are presented in Fig. 4. The SEM images of $La_{0.90}K_{0.10}CoO_3$ perovskite-type oxides show that the catalyst particles had average particle sizes centered around 60–100 nm with a spherical shape. For comparison, the SEM photographs of the $La_{0.9}K_{0.1}CoO_3$ sample after being compressed and sieved or the sample synthesized by solid phase mechanically mixed method are also shown in Fig. 4. The results indicate that the particle sizes of the $La_{0.9}K_{0.1}CoO_3$ sample after being compressed and sieved became larger and their shapes are similar to strip. Moreover, the size distribution of the sample synthesized by solid phase mechanically mixed method is more irregular. In other words, some particle sizes of the samples obtained by solid phase mechanically mixed method are much bigger than those of the sample obtained with citric acid-ligated method, while some particle sizes are small and their sizes are similar to those of the sample obtained with citric acid-ligated method. This change of the particle sizes and dispersion of catalysts might lead to the lower catalytic activity for the simultaneous removal of soot and NO_x.

3.5 XPS Results

XPS spectra of $La_{1-x}K_xCoO_3$ for Co2p are shown in Fig. 5. The binding energies of $Co2p_{3/2}$ for $LaCoO_3$, $La_{0.90}K_{0.10}CoO_3$ and $La_{0.70}K_{0.3}CoO_3$ are 779.0, 779.5 and 779.0 eV, respectively. The binding energy of $Co2p_{3/2}$ in Co_2O_3, Co_3O_4 and CoO oxides were 779.6, 779.8 and 780.4 eV, respectively. The binding energy of $Co2p_{3/2}$ in $La_{1-x}K_xCoO_3$ is much lower than that in simple oxides. This result is very consistent with the founding by Zhu et al. [17] and the binding energy of $Co2p_{3/2}$ in $LaCoO_3$ was 778.8 eV in their study. Due to the XPS peaks of these three samples for $Co2p_{3/2}$ are not symmetric, these XPS profiles were fit by a standard Gaussian deconvolution method to get a relative content of Co corresponding to low and high binding energy. The deconvolution analysis results are listed in Table 2. The peak area ratio of $Co2p_{3/2}$ with high binding energy to that with low binding energy is much greater than that of unsubstituted sample of $LaCoO_3$. Moreover, this area ratio increases with the increasing the K-substitution amount. These results demonstrate that the content of Co ion with higher oxidation state increases with the increasing of K-substitution amount. In the unsubstituted $LaCoO_3$ perovakite-type complex oxide, the normal oxidation state of Co ion should be +3. Thus some amounts of Co^{3+} may change into Co^{4+} to make the charge balance when K^+ was introduced into $LaCoO_3$ to partially replace La^{3+} [16, 18, 19].

There were mainly two chemical states of oxygen in the $La_{1-x}K_xCoO_3$ oxides and they can be fitted into two oxygen species as shown in Fig. 6 and Table 3. The peak with a low binding energy (~528.5 eV) was assigned to the lattice oxygen. Another one with a high binding energy (~530.8 eV) was attributed to the adsorbed oxygen in oxygen vacancy of this kind of defect oxides [17–20]. For $LaCoO_3$ sample, the area ratio of $O_{ads}/O_{lat.}$ is close to 1. The ratio of K-substituted sample is much greater than that of the unsubstituted sample $LaCoO_3$. And it increases with the increasing of K-substitution amount. These results strongly demonstrate that some amounts of oxygen vacancy may form when some amounts of K^+ was introduced into $LaCoO_3$ to partially replace La^{3+}.

3.6 Catalytic Activity for the Simultaneous Removal of Soot and Nitrogen Oxides

Figure 7 shows the results of the temperature-programmed oxidation reaction over $LaCoO_3$. The formation of carbon dioxide and carbon monoxide due to the oxidation of the soot and the reduction of NO_x to nitrogen took place in the same temperature range, evidencing the occurrence of the simultaneous removal of NO_x and soot [2–5]. The sudden drop of carbon dioxide and carbon monoxide and nitrogen formation at higher temperature is, of course, due to the exhaustion of the charged soot. From the temperature-programmed oxidation results, the parameters were derived in order to evaluate the catalytic performance. One is the ignition temperature of the soot (T_{ig}) estimated by extrapolating the steeply ascending portion of the carbon dioxide formation curve to zero carbon dioxide concentration, and the second one was the temperature corresponding to the soot maximal combustion rate (T_m) and the third one was the final combustion temperature (T_f) obtained by extrapolating the steeply descending portion of the carbon dioxide formation curve to zero carbon dioxide concentration [2–4]. The last one is the maximal conversion of nitrogen oxide (X_{NO}) to nitrogen molecule for the simultaneous removal of soot and nitrogen oxides. A good catalyst should be the oxide with low T_{ig} and large X_{NO}. The X_{NO} was defined as:

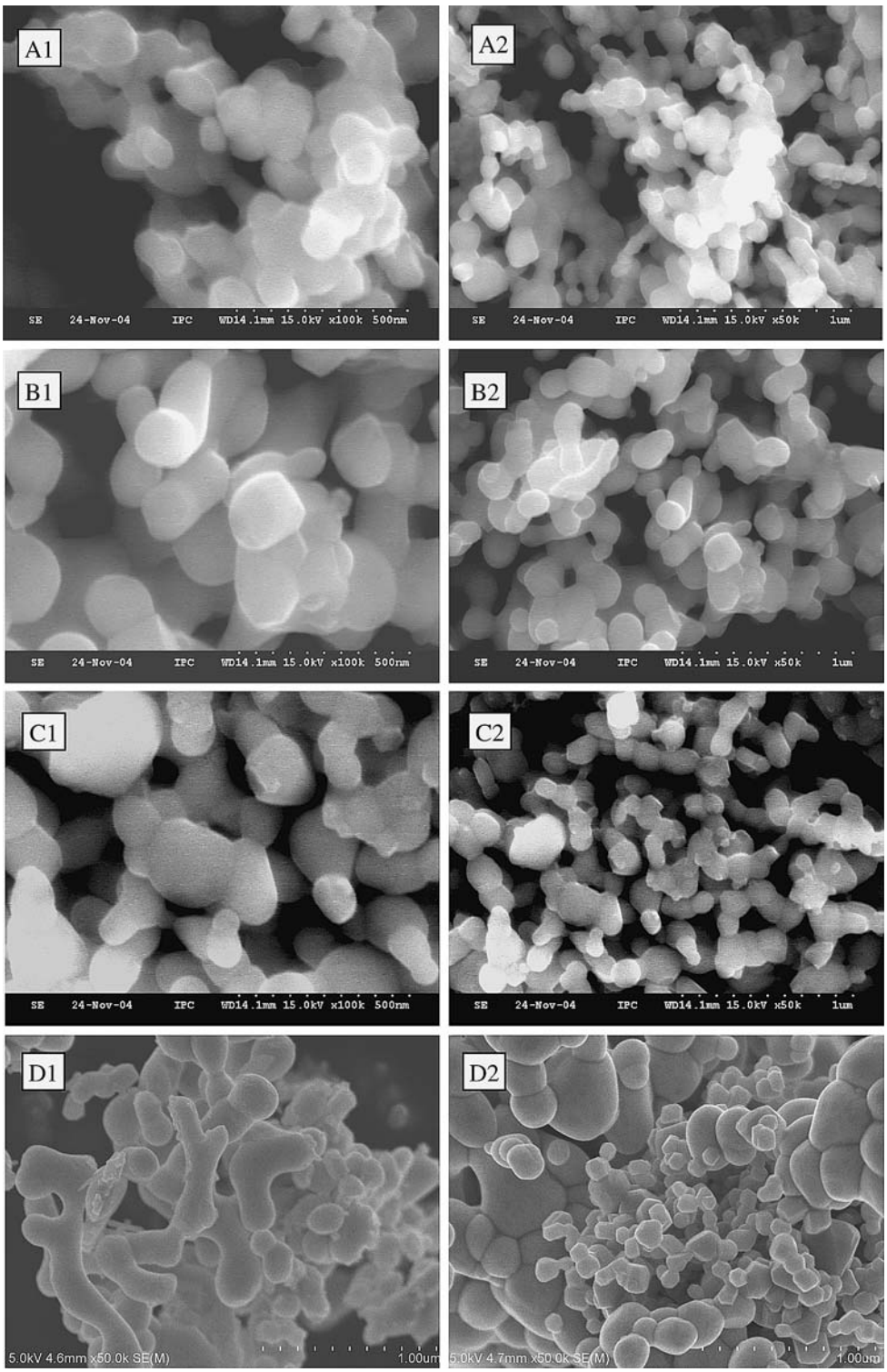

Fig. 4 SEM photographs of $La_{1-x}K_xCoO_3$ catalysts. A1,A2: $LaCoO_3$; B1,B2: $La_{0.95}K_{0.05}CoO_3$; C1,C2: $La_{0.90}K_{0.10}CoO_3$. D1: $La_{0.90}K_{0.10}CoO_3$ (180–230 μm), D2: $La_{0.90}K_{0.10}CoO_3$ (solid phase mechanically mixed)

$$X_{NO}\% = \frac{[NO]_{N_2}}{[NO]_{in}} \times 100 = \frac{2[N_2]_{out}}{[NO]_{in}} \times 100$$

$[NO]_{in}$ is NO mole concentration in the inlet gases, ppm, and $[N_2]_{out}$ is N_2 molar concentration in outlet gas, ppm.

Due to the importance of the T_{ig} in reflecting the nature of catalytic activity of the studied catalysts for soot oxidation the T_{ig} was selected as judging criteria in several pioneer and previous reports by Teraoka [2–4, 8] and Seong-Soo Nong [5]. So T_{ig} was also chosen as the

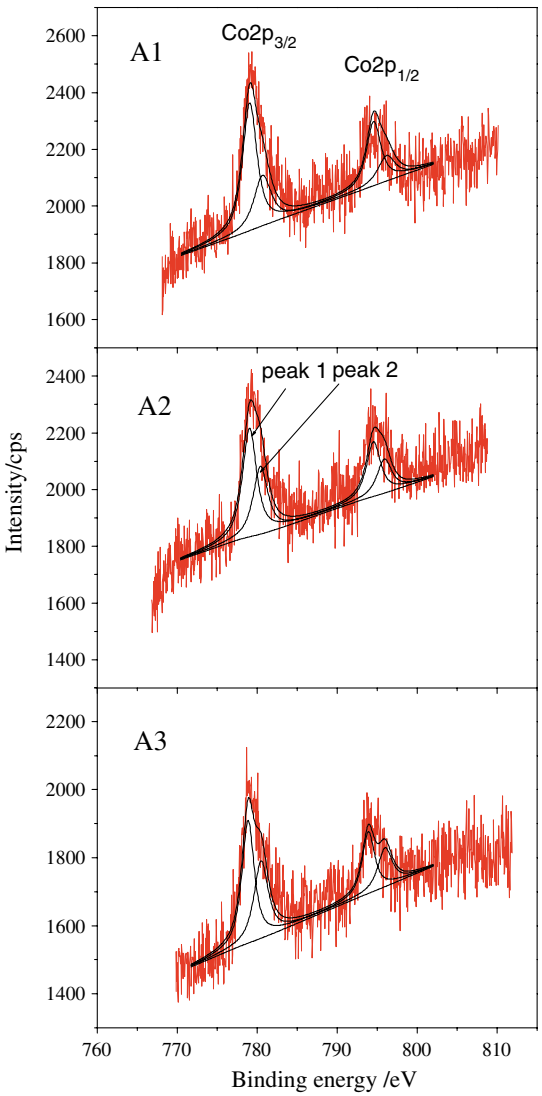

Fig. 5 XPS spectra for Co2p of $La_{1-x}K_xCoO_3$ oxides. A1: $LaCoO_3$; A2: $La_{0.90}K_{0.10}CoO_3$; A3: $La_{0.70}K_{0.30}CoO_3$

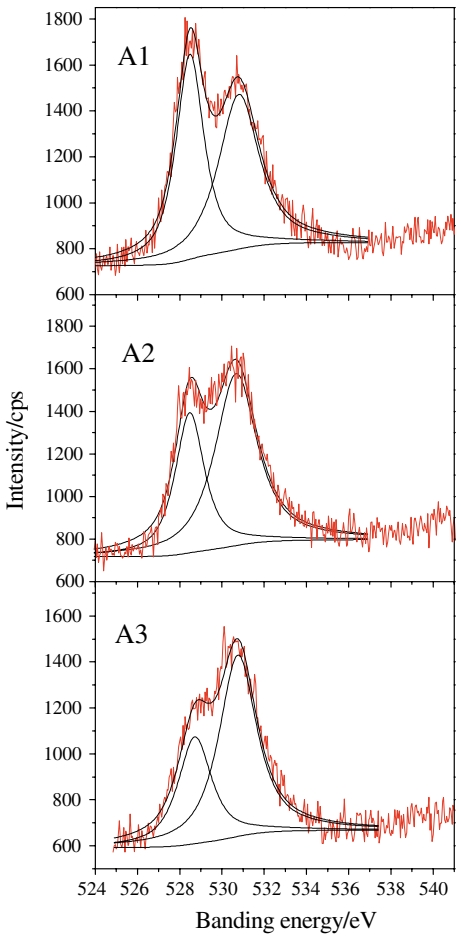

Fig. 6 XPS spectra for O_{1s} of $La_{1-x}K_xCoO_3$ oxides. A1: $LaCoO_3$; A2: $La_{0.90}K_{0.10}CoO_3$; A3: $La_{0.70}K_{0.30}CoO_3$

main judging criterion for soot oxidation reaction in this study.

The TPR results (in Tables 4 and 5) show that the soot combustion temperature significantly reduced and the conversion X_{NO} largely increased over all the K^+-substitution samples compared to the unsubstituted sample $LaCoO_3$. T_{ig} almost slowly decreases with the increasing of K-substitution amount and the sample with potassium substitution amount of $x = 0.3$ has the lowest T_{ig} and T_f. The catalytic performances of the samples with $x = 0.1$–0.3 are not so much different if T_m and T_f are also used as the judging criteria. However, as shown in Table 5, the temperatures of those ignitions slightly change with the particle size, but the changes of T_m and T_f are much bigger. It is because that soot combustion is solid–solid–gas triple phase complex reactions. The contact between catalytic sites and soot, is of great importance for solid–solid reactions. T_{ig} reflects the intrinsic nature of catalyst, however T_m and T_f are also closely related to the contact between catalyst and soot. Once the ignition takes place, the contact condition becomes important. The difference between T_{ig} and T_m, T_f from Tables 4 and 5 can be taken as a measure of the nature of the catalytic site versus the number of

Table 2 The binding energy of $Co2p_{3/2}$ in $La_{1-x}K_xCoO_3$ oxides

Catalysts	Peak	Peak 1		Peak 2		Peak 2/Peak 1
	Position (eV)	Position (eV)	Area	Position (eV)	Area	
$LaCoO_3$	779.0	779.0	2,138.30	780.4	1,007.25	0.47
$La_{0.90}K_{0.10}CoO_3$	779.5	779.0	1,775.66	780.4	1,150.96	0.65
$La_{0.70}K_{0.30}CoO_3$	779.0	778.9	1,477.38	780.5	1,060.90	0.72

Table 3 The composition of surface oxygen species in $La_{1-x}K_xCoO_3$ oxides

Catalysts	O_{lat}			O_{ads}			O_{ads}/O_{lat}
	Position (eV)	Area	FWHM (eV)	Position (eV)	Area	FWHM (eV)	
$LaCoO_3$	528.5	2,077.87	1.584	530.8	2,257.77	2.283	1.09
$La_{0.90}K_{0.10}CoO_3$	528.5	1,604.49	1.657	530.7	2,801.64	2.359	1.75
$La_{0.70}K_{0.30}CoO_3$	528.7	1,304.44	1.908	530.8	2,460.99	2.123	1.89

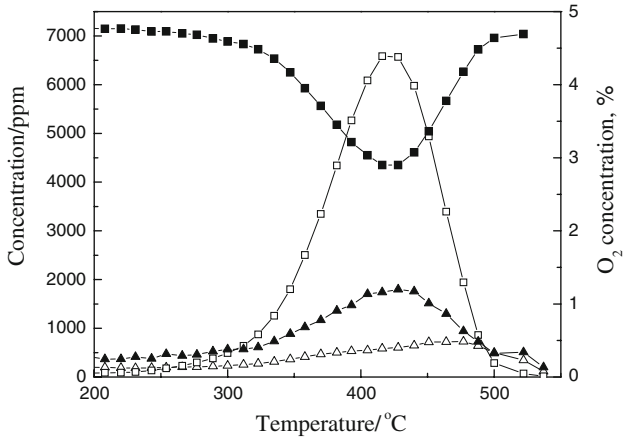

Fig. 7 TPR profiles for the simultaneous removal of soot and NO_x over $LaCoO_3$ catalysts. ■: O_2; □: CO_2; ▲: N_2*10; △: CO*10

contact points between these sites and soot. A small difference indicates a very good contact between soot and catalyst. Once the nucleus ignites, the oxidation of soot proceeds quickly. A large difference between T_{ig} and T_m or T_f indicates poor contact and once ignition takes place, depending on the nature of the site, the oxidation process proceeds rather slowly. Moreover, X_{NO} for potassium substitution amount of $x = 0.3$ is relatively high. Therefore, this catalyst should be the best catalyst among the studied catalysts.

The catalytic performance of pure Co_3O_4 sample for soot oxidation under same conditions was also investigated (Table 4). Simple oxide of Co_3O_4 possessed good catalytic performances for soot oxidation, while it is much less active than those of La–K–Co–O perovskite oxides, especially Co_3O_4 has special pattern for soot oxidation. For example it gave two broad TPR peaks, i.e., two T_m and very high T_f. Although we could not exclude the tiny contribution of the impurity of Co_3O_4 to the soot oxidation activity, it is clear the catalytic performance of the La–K–Co–O perovskite oxide catalyst was mainly contributed by the phase of La–K–Co–O perovskite complex oxide by comparing the catalytic behaviours of La–K–Co–O sample and pure Co_3O_4.

Table 4 The combustion temperature of soot and the conversion of NO for the simultaneous soot and NO_x over $La_{1-x}K_xCoO_3$ oxides

Catalyst	T_{ig} (°C)	T_m (°C)	T_f (°C)	X_{NO} (%)	S_{CO_2} (%)
No catalyst	460	599	655	9.9	65.2
Co_3O_4	307	410, 508	549		
$LaCoO_3$	324	421	496	17.2	99.1
$La_{0.95}K_{0.05}CoO_3$	303	408	472	29.9	98.8
$La_{0.90}K_{0.10}CoO_3$	298	398	463	36.0	98.3
$La_{0.85}K_{0.15}CoO_3$	294	415	468	34.9	98.9
$La_{0.80}K_{0.20}CoO_3$	296	410	462	36.1	98.4
$La_{0.75}K_{0.25}CoO_3$	294	408	480	40.4	98.4
$La_{0.70}K_{0.30}CoO_3$	289	400	461	34.6	98.4

The $La_{0.70}K_{0.30}CoO_3$ oxides are good candidate catalysts for the simultaneous removal of soot and nitrogen oxides, and the combustion temperatures of soot particle are as low as those between 289 and 461 °C, the NO_x conversion to N_2 is 34.6% when the contact between catalysts and soot is loose. For comparison, Table 5 lists the combustion temperature of soot and the conversion of NO for the simultaneous removal of soot and NO_x over $La_{0.9}K_{0.1}CoO_3$ catalyst with different particle sizes or prepared by the different methods. The results indicate that the temperatures of soot combustion over samples with lager sizes were much higher than those of soot oxidation over nanometric catalysts. It indicates that the particle sizes of catalysts and preparation method remarkably affected on their catalytic performances for the simultaneous removal of soot and NO_x.

3.7 The Probable Reasons that Can Lead to the Activity Enhancement for K^+-substitution

For perovskite-type oxide catalyst, B-site cations for soot combustion possess the function of catalysis. The cation at

Table 5 The combustion temperature of soot and the conversion of NO for the simultaneous soot and NO_x over $La_{0.9}K_{0.1}CoO_3$ catalyst with different sizes or prepared by the different methods

Catalyst	T_{ig} (°C)	T_m (°C)	T_f (°C)	X_{NO} (%)	S_{CO_2} (%)
$La_{0.9}K_{0.1}CoO_3$ (60–100 nm)	298	398	463	36	98
$La_{0.9}K_{0.1}CoO_3$ (180–230 μm)	303	410	498	31	95
$La_{0.9}K_{0.1}CoO_3$ (380–830 μm)	311	427	544	20	95
$La_{0.9}K_{0.1}CoO_3$ (solid phase mechanically mixed method, 180–230 μm)	328	406	525	31	89

A-site (La^{3+}) is generally trivalent, as La^{3+} at A-site is replaced by lower valency cation K^+, according to the principle of electron neutrality, the positive charge reduced could be balanced either by the formation of higher oxidation state ion at B-site [19–23], i.e.,

$$Co^{3+} \rightarrow Co^{4+}$$

$$La_{1-x}K_xCo^{3+}_{1-2x}Co^{4+}_{2x}O_3 \rightarrow LaCoO_3 + xLa^{3+}|K^+|'' + 2x\ Co^{3+}|Co^{4+}|^{\bullet}$$

or by the formation of oxygen vacancy (V_0) in $La_{1-x}K_xCoO_3$.

$$La_{1-x}K_x\lambda(V_0)Co^{3+}O_{3-\lambda} \rightarrow LaCoO_3 + xLa^{3+}|K^+|'' + \lambda|O|^{\bullet\bullet}$$

In addition to the both cases discussed above, a small amount of B-site vacancy may be formed due to the large difference in valance between K^+ and La^{3+}. This consideration was confirmed by the formation of a small amount of Co_3O_4 detected by IR and XRD measurements when a large amount of K^+ was introduced into $LaCoO_3$ for the substitution of La^{3+}.

Based on the above discussion, the following three reasons can lead to the activity enhancement for K-substituted samples ($La_{1-x}K_xCoO_3$) compared to the unsubstituted sample ($LaCoO_3$). The first one is that A-site cation (La^{3+}) was partly replaced by K^+ and partial Co^{3+} changed to Co^{4+}, which had better catalytic oxidation activity than Co^{3+}. The second one is the increase in the content of oxygen vacancy (V_0) in $La_{1-x}K_xCoO_3$. Generally, the adsorption of NO by perovskite oxides is related to the surface area and oxygen vacancies. The surface areas of all perovskite catalysts are small due to calcinations at high temperature. Thus, the difference in adsorbed amount of NO on different catalysts would be attributed to the different concentrations of oxygen vacancies. The XPS results demonstrate that the content of surface adsorbed oxygen and oxygen vacancy concentration of $La_{1-x}K_xCoO_3$ oxide catalysts increase with increasing in the K-substituted amount for La. The presence of a large amount of oxygen vacancies would accelerate the mobility of lattice oxygen and facilitate to the reproduction of oxygen vacancy, which increases the adsorption and activation of NO or molecular oxygen of catalyst surface. Therefore, it can improve the catalytic activity for simultaneous removal NO_x and soot. Thus, the catalytic activities of the K-substituted catalysts were further improved. The last one is that the nanoparticle $La_{1-x}K_xCoO_3$ perovskite-type oxides were obtained. The surface particle sizes of nanoparticle catalyst are small. Surface atoms on the nanoparticle catalysts have extra and high surface energies and they are good at mobility, therefore the contact is still very good between catalysts and soot even under loose contact conditions. The results in Table 5 support this point of view. The sample synthesized by solid phase mechanically mixed method has lower catalytic activity for the simultaneous removal of soot and NO_x because of their larger particle sizes.

4 Conclusions

The nanoparticle $La_{1-x}K_xCoO_3$ perovskite-type oxides were obtained by the citric acid-ligated method. The diesel soot and NO_x could be simultaneously removed over the $La_{1-x}K_xCoO_3$ oxide catalysts and the partial substitution of La^{3+} at A-site by alkali metal K^+ enhanced the catalytic activity for the oxidation of soot particle and reduction of NO_x. Three possible reasons, i.e., the formation of high valance ion (Co^{4+}) at B-sites, the formation of oxygen vacancy, and the formation of oxide catalysts with nanometric size and thus the good contact between the catalysts and soot, are considered for the activity enhancement in the reaction of simultaneous removal of diesel soot and nitrogen oxides when some amounts of La^{3+} at A-sites were replaced by K^+. Especially, the particle size has a large effect on their catalytic performances of studied catalysts for the simultaneous removal of diesel soot and nitrogen oxides. The superior activities of the $La_{0.70}K_{0.30}CoO_3$ catalyst for the title reaction can be obtained. The oxidation temperature for soot particle over the $La_{0.70}K_{0.30}CoO_3$ catalyst is between 289 and 461 °C, the selectivity of CO_2 is 98.4% and the conversion of NOx to N_2 is 34.6% under loose contact conditions.

Acknowledgments This work was supported by the National Natural Science Foundation of China (No. 20773063, 20525621 and 20473053), the Beijing Natural Science Foundation (No. 2062020), the 863 Program of China (No.2006AA06Z346) and the Scientific Research Key Foundation for the Returned Overseas Chinese Scholars of State Education Ministry.

References

1. Pisarello ML, Milt V, Peralta MA, Querini CA, Miró EE (2002) Catal Today 75:465
2. Teraoka Y, Nakano K, Kagawa S, Shangguan WF (1995) Appl Catal B 5:L181
3. Teraoka Y, Nakano K, Shangguan WF, Kagawa S (1996) Catal Today 27:107
4. Shangguan WF, Teraoka Y, Kagawa S (1998) Appl Catal B 16:149
5. Hong SS, Lee G-D (2000) Catal Today 63:397
6. Fino D, Fino P, Saracco G, Specchia V (2003) Appl Catal B 43:243
7. Miyazaki T, Tokabuchi N, Arita M, Inoue M, Mochida I (1997) Energy Fuel 11:832
8. Teraoka Y, Kanada K, Kagawa S (2001) Appl Catal B 34:73
9. Neeft JPA, Michiel M, Jacob A (1996) Appl Catal B 8:57
10. Zhao Z, Obuchi A, Oi-Uchisawa J, Ogata A, Kushiyama S (1998) Chem Lett 4:367
11. Liu ST, Obuchi A, Uchisawa J, Nanba TA, Kushiyama S (2002) Appl Catal B 37:309

12. Carrascull A, Lick ID, Ponzi EN, Ponzi EN, Ponzi MI (2003) Catal Commun 4:124
13. Liu J, Zhao Z, Xu C, Duan A, Zhu L, Wang X (2005) Appl Catal B 61:36
14. Lik KB, Li XJ, Zhu KG (1997) J Appl Phys 10:6943
15. Couzi M, Huong PV (1974) Anal Chem 9:19
16. Merino NA, Barbero BP, Grange P, Cadus LU (2005) J Catal 231:232
17. Tan RQ, Zhu YF (2005) Appl Catal B 58:61
18. Wu Y, Wu T, Dou BS, Wang CX, Xie XF, Yu ZL, Fan SR, Fan ZR, Wang LC (1989) J Catal 120:88
19. Zhao Z, Yang X, Wu Y (1996) Appl Catal B 8:281
20. Cruz RMG, Falcon H, Pena MA, Fierro JLG (2001) Appl Catal B 33:45
21. Wang H, Zhao Z, Xu C, Liu J (2005) Catal Lett 102:251
22. Liu J, Zhao Z, Xu C, Duan A (2008) Appl Catal B 78:61
23. Liu J, Zhao Z, Xu C, Duan A, Meng T, Bao X (2007) Catal Today 119:267